

The Lissajous lens: a three-dimensional absolute optical instrument without spherical symmetry

Aaron J. Danner,^{1,*} H. L. Dao,¹ and Tomáš Tyc²

¹Department of Electrical and Computer Engineering,
National University of Singapore, 4 Engineering Drive 3, 117583 Singapore

²Faculty of Science and Faculty of Informatics,
Masaryk University, Kotlářská 2, 61137 Brno, Czech Republic

*adanner@nus.edu.sg

Abstract: We propose a three dimensional optical instrument with an isotropic gradient index in which all ray trajectories form Lissajous curves. The lens represents the first absolute optical instrument discovered to exist without spherical symmetry (other than trivial cases such as the plane mirror or conformal maps of spherically-symmetric lenses). An important property of this lens is that a three-dimensional region of space can be imaged stigmatically with no aberrations, with a point and its image not necessarily lying on a straight line with the lens center as in all other absolute optical instruments. In addition, rays in the Lissajous lens are not confined to planes. The lens can optionally be designed such that no rays except those along coordinate axes form closed trajectories, and conformal maps of the Lissajous lens form a rich new class of optical instruments.

© 2015 Optical Society of America

OCIS codes: (080.2710) Inhomogeneous optical media; (080.2740) Geometric optical design; (080.5692) Ray trajectories in inhomogeneous media.

References and links

1. U. Leonhardt, "Optical conformal mapping," *Science* **312**, 1777-1780 (2006).
2. J. B. Pendry, D. Schurig, and D. R. Smith, "Controlling electromagnetic fields," *Science* **312**, 1780-1782 (2006).
3. U. Leonhardt and T. Tyc, "Broadband invisibility by non-Euclidean cloaking," *Science* **323**, 110-112 (2009).
4. M. Born and E. Wolf, *Principles of optics* (Cambridge University, 2006).
5. J. C. Miñano, "Perfect imaging in a homogeneous three-dimensional region," *Opt. Express* **14**, 9627-9635 (2006).
6. T. Tyc, L. Herzánová, M. Šarbort, and K. Bering, "Absolute instruments and perfect imaging in geometrical optics," *New J. Phys.* **13**, 115004 (2011).
7. R. K. Luneburg, *Mathematical theory of optics* (University of California, 1964).
8. T. Tyc and A. J. Danner, "Frequency spectra of absolute optical instruments," *New J. Phys.* **14**, 085023 (2012).
9. T. Tyc, "Spectra of absolute instruments from the WKB approximation," *New J. Phys.* **15**, 065005 (2013).
10. H. Goldstein, C. Poole, and J. Safko, *Classical mechanics* (Addison-Wesley, 2001).
11. U. Leonhardt and T. Philbin, *Geometry and light: The science of invisibility* (Dover, Mineola, 2010).
12. M. Šarbort and T. Tyc, "Spherical media and geodesic lenses in geometrical optics," *J. Opt.* **14**, 075705 (2012).

1. Introduction

The advent of transformation optics [1, 2] and recent efforts to construct useful non-Euclidean lenses [3] have brought increased attention to the field of gradient index lens design. In this

paper, we show that the field of absolute optical instruments, a special subset of non-Euclidean gradient index lenses, is richer than previously realized.

An absolute optical instrument is a region of space filled with an optical medium where all points are imaged stigmatically. In other words, light rays emanating from a single point anywhere in space will, at some later time, all converge to a single point in space. The well-known textbook by Max Born and Emil Wolf [4] discusses the two then-known examples of absolute optical instruments, the plane mirror (which creates virtual images of all points in half-space), and the Maxwell Fisheye (which creates real images of all points in space). It was recently discovered that there is an infinite number of absolute optical instruments of both categories, and many properties of these lenses, as well as techniques for determining the refractive index profiles of them, are now known [5, 6]. Nonetheless, there are still many open questions; for example, is there a formulaic way of constructing all possible absolute optical instruments?

2. The Lissajous lens

Absolute optical instruments possess interesting properties, both in terms of ray behavior and in wave optics. Rays, for example, spreading out from any point A in space will later converge at point B in space (which may happen to be the same point as A). Examples of this behavior of rays are shown in Fig. 1(a) for the Maxwell fisheye and in Fig. 1(b) for the Luneburg [7] lens. This property of diverging and converging rays extends to wave optics as well; waves diverging from a dipole point source in an absolute optical instrument all later converge. It has been shown [8, 9] that this behavior is closely related to the properties of the spectrum of absolute instruments which is highly degenerate and almost evenly spaced; this tends to keep optical pulses from spreading out. In the lens presented in this paper that we will refer to as the Lissajous lens, as we shall see, the degeneracy and even spacing of the spectrum is perfect, and optical pulses have a soliton-like property when propagating within such a cavity, never spreading out but periodically oscillating in shape.

The proposed Lissajous lens is an optical analogue of an anisotropic mechanical harmonic oscillator. To explain the properties of the lens, we start with the oscillator and then proceed to the optical case.

The Lagrangian of the anisotropic oscillator with mass m is given by

$$L = \frac{m}{2}(\dot{x}^2 + \dot{y}^2 + \dot{z}^2) - \frac{\mathcal{E}}{2} \left(\frac{x^2}{a^2} + \frac{y^2}{b^2} + \frac{z^2}{c^2} \right), \quad (1)$$

where \mathcal{E} is a constant with the dimension of energy and a , b , and c are constants with the dimension of length representing the anisotropy of the potential in the three Cartesian directions. Clearly, the Lagrangian of the system is separable in Cartesian coordinates. This leads to independent harmonic oscillations in the three spatial directions; for example, $x(t) = A_x \cos(\omega_x t - \phi_x)$, where A_x and ϕ_x are constants depending on the initial conditions, and $\omega_x^2 = \mathcal{E}/(ma^2)$. The combination of the three harmonic motions results in a trajectory with the form of a three-dimensional (3D) extension of the well-known Lissajous curve [10]. (We will use the term “Lissajous curve” throughout this paper although the 3D version of the curve is usually called “Lissajous knot”.)

3. Ray propagation inside the Lissajous lens and its geodesic equivalence

To proceed to the construction of Lissajous lens, we employ the close relationship between classical mechanics and geometrical optics [11]. The geometrical shape of particle trajectories with the Lagrangian (1) and energy E are the same as trajectories of light rays in a medium with refractive index proportional to $\sqrt{2(E - V)}$, where V is the potential energy. Setting the

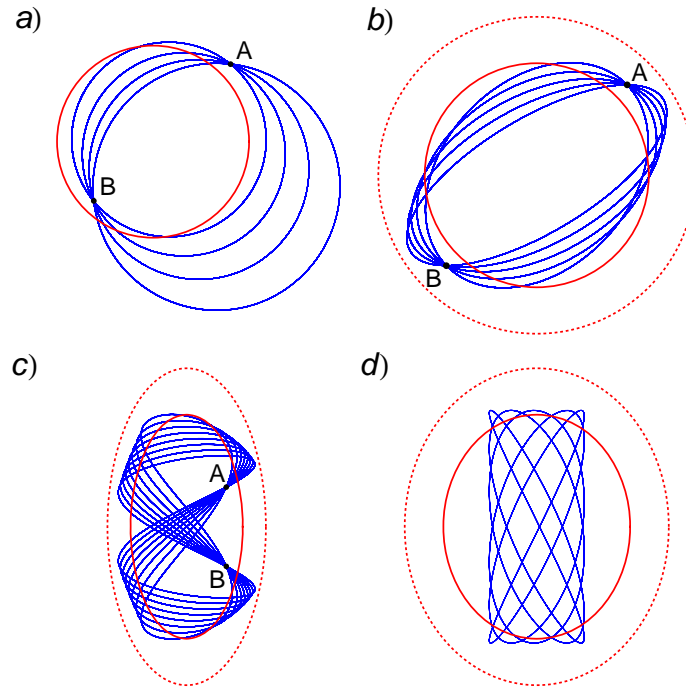


Fig. 1. Ray trajectories in a) Maxwell's fisheye, b) the Luneburg lens, c) a Lissajous lens with $a = 1$, $b = 2$, and d) a Lissajous lens with $a = 5/3$, $b = 2$. The solid simple curves represent the line on which $n = 1$ in the optical case, and the outer dotted lines represent the $n = 0$ lens boundary. In (a–c), points A and B represent example source and image, respectively.

energy E to \mathcal{E} , this leads to the refractive index distribution

$$n(x,y,z) = \sqrt{2 - \left(\frac{x}{a}\right)^2 - \left(\frac{y}{b}\right)^2 - \left(\frac{z}{c}\right)^2}; \quad (2)$$

the index is equal to unity at the surface of the ellipsoid with the semiaxes a, b , and c . From the analogy with mechanics it then immediately follows that the ray trajectories in this index are also given by Lissajous curves. Figures. 1(c) and 1(d) show example ray trajectories in two two-dimensional (2D) lenses for two different a -to- b ratios. It can be seen clearly in Fig. 1(c) that light emerging from one point later converges to another, and this property is true for light emanating from any point within the lens, so long as the ratio of a and b is rational. Note that the image points do not have to lie on a straight line with the center of the lens [6], a property likely unique to this lens (excepting conformal inversions of other reported lenses). Figure 2(a) shows an example of a 3D Lissajous lens and again illustrates its unique imaging property. Figure 2(b) shows an example lens where ray trajectories become helical if one of the parameters a, b or c goes to infinity.

In the language of transformation optics [11], the refractive index (2) of the Lissajous lens creates an effective non-Euclidean geometry for light rays that follow geodesic curves with respect to this geometry. In the case of the 2D lens, this geometry can be visualized by embedding a certain 2D non-Euclidean surface into 3D space; ray trajectories are then represented by geodesics on this surface. Mathematically, this means that the profile $n(x,y)$ is equivalent to a

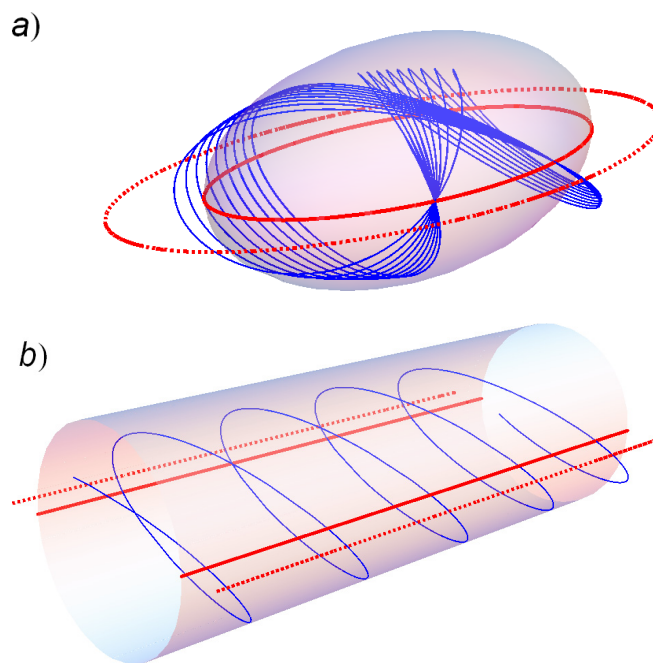


Fig. 2. a) Lissajous lens with $a = 1$, $b = 2$, $c = 1$, b) Lissajous-like lens with $a = 1$, $b \rightarrow \infty$, $c = 1$. The surface plots are the surfaces of unity index. The full red lines mark intersections of these surfaces with the xy plane while the dotted red lines mark the places in this plane where $n = 0$.

surface $\mathcal{S}(x, y, z)$ with $n = 1$ homogeneously. Every refractive index profile has an equivalent non-Euclidean surface, which is called its geodesic lens. The geodesic lenses can be obtained analytically for spherically symmetric profiles as done in [12]; but for profiles without spherical symmetry, it is exceedingly hard to obtain analytical solutions. For this reason, we have developed numerical methods to generate the surface shown in Fig. 3; although infinitely many solutions are possible, it was a computationally complex task to numerically find even a single solution.

Specifically, we generated the surface by a numerical optimization procedure using the built-in algorithm `NMinimize` of the software `Mathematica`, which gives the explicit coordinates (x_i, y_i, z_i) of points P_i with $i = 1, 2, \dots, N$, (where N is the number of points used in the numerical grid) belonging to the geodesic lens surface at the end of the optimization process. To obtain this, we made the set of all unknown coordinates (x_i, y_i, z_i) to be the variables with respect to which a certain object is optimized. The object to be optimized is the sum of the distances $\sum d_{ij}$ between neighboring points P_i, P_j on the surface of the geodesic lens, together with a set of constraints designed to get a sensible result. The constraints used are: Firstly, the individual distances d_{ij} must match the corresponding optical paths in the 2D optical profile as closely as possible; and secondly, the surface must be smooth (having approximately the same curvature throughout).

For 2D refractive index profiles with the boundary $n = 0$ at $r = \sqrt{x^2 + y^2} \rightarrow \infty$ like that of the Maxwell fisheye's, the equivalent geodesic lenses have two parts: an upper part with $z > 0$ corresponding to $n \geq 1$ and a lower part with $z < 0$ corresponding to $0 \leq n < 1$; the surfaces nicely close at $n = 0$ (or at $r \rightarrow \infty$). However, for refractive index profiles that have $n = 0$ at

a finite distance from the origin like that of the Luneburg ($r = \sqrt{2}$) or Eaton ($r = 2$) lenses, the lower parts of the geodesic lenses can only be partially constructed as the coordinate z will become complex at some value of n close to, but smaller than 1 [12]. Unfortunately, the same thing happens with the 2D Lissajous profile, which has finite values of x and y at $n = 0$; thus it is impossible to fully construct a geometrical representation of the required surface in 3D Euclidean space and still maintain a real-valued z -coordinate when $0 \leq n \lesssim 0.85$. The surface shown in Fig. 3 corresponds to the inner part of the lens where $n > 1$, and is the geodesic-lens-equivalence of the lens shown in Fig. 1(c). In both Fig. 3 and Fig. 1(c), the two image points are visible.

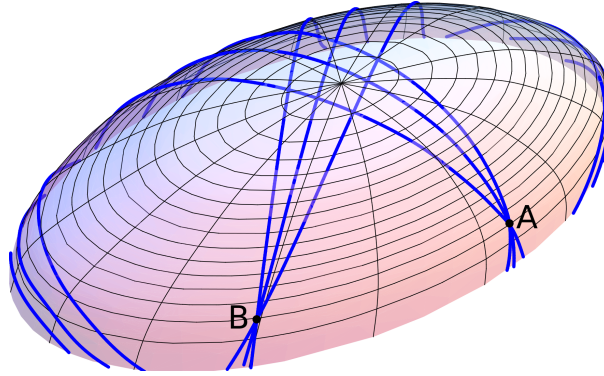


Fig. 3. Equivalent geodesic surface to a Lissajous lens with $a = 1$, $b = 2$ for the region of the lens where $n \geq 1$.

4. Wave properties of the Lissajous lens

Lastly, we will describe the wave-optical properties of the Lissajous lens. For simplicity, we will consider scalar waves instead of the full vector description in terms of Maxwell's equations. In the wave equation $C^2 \Delta \psi - n^2 \psi_{tt} = 0$, where C is the speed of light, all the variables can be separated to give the solution in the form $\psi(x, y, z, t) = \psi_x(x) \psi_y(y) \psi_z(z) \cos(\omega t - \phi)$. The (unnormalized) functions $\psi_{x,y,z}$ are scaled Hermite Gaussians,

$$\begin{aligned}\psi_x(x) &= H_n(x \sqrt{k/a}) e^{-kx^2/(2a)} \\ \psi_y(y) &= H_m(y \sqrt{k/b}) e^{-ky^2/(2b)} \\ \psi_z(z) &= H_p(z \sqrt{k/c}) e^{-kz^2/(2c)}\end{aligned}\quad (3)$$

where

$$k = \frac{\omega}{C} = \frac{n+1/2}{a} + \frac{m+1/2}{b} + \frac{p+1/2}{c}\quad (4)$$

with n , m , and p non-negative integers, and H_n denoting the Hermite polynomial. If the ratios a/b , b/c , and a/c are rational, then it is not hard to show that all the eigenfrequencies are integer multiples of $\omega_0 = C/(2d)$, where d is the least common multiple of a, b, c (i.e., the smallest value for which $d/a, d/b, d/c$ are all integers). This implies that an arbitrary wave in such a Lissajous lens is periodic with period $T_0 = 2\pi/\omega_0$. Hence if a pulse of light is emitted from any point within the lens, some time later the wave will be exactly the same as it was when released. This means that an arbitrary point A is an image of itself, and depending on the ratios of a, b , and c , there may exist also intermediate images (such as point B in Fig. 1(c)).

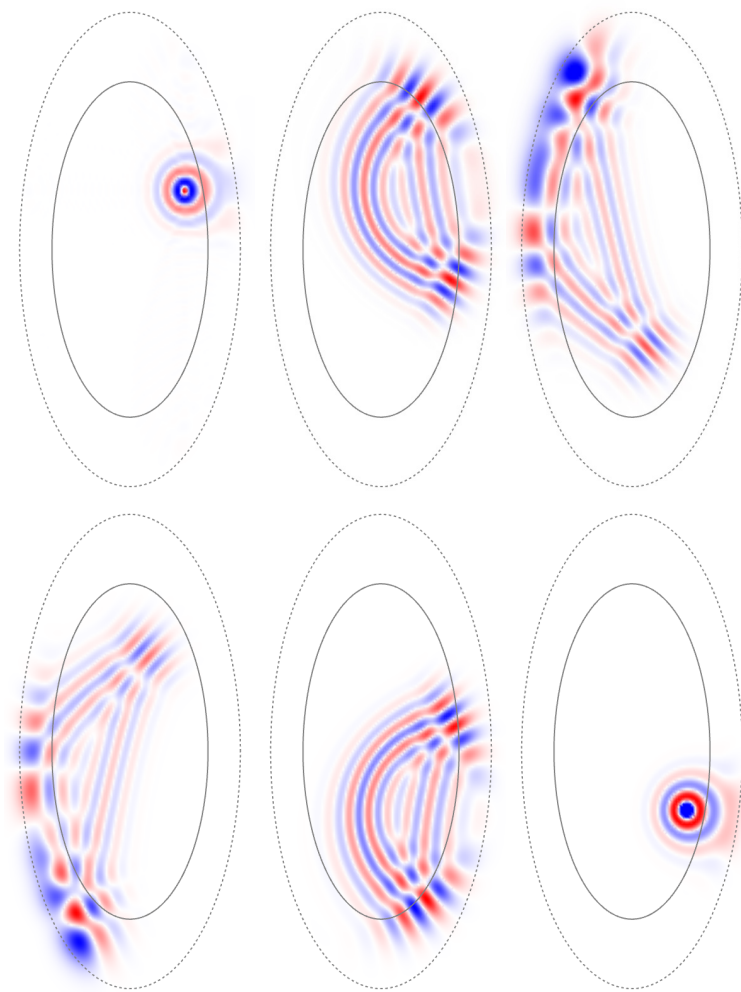


Fig. 4. Time evolution of a Gaussian pulse propagating in a Lissajous lens with $a = 1$, $b = 2$, illustrating stigmatic imaging.

The fact that all the eigenfrequencies are integer multiples of $\omega_0 = C/(2d)$ also means that the frequency spectrum has behavior typical for absolute instruments – it is highly degenerate with equidistantly spaced groups [8, 9]. This is in particular obvious for Luneburg lens for which $a = b = c$ and all the eigenfrequencies are of the form $\omega = (N + 1/2)C/a$ with N integer. Moreover, the degeneracy and equidistance of the spectrum of Lissajous lenses is perfect, in contrast to some other absolute instruments where it is only approximate [8, 9].

Figure 4 shows that a Gaussian pulse initially emitted from one point will later reform at the image point. This means that sharp, aberration-free imaging by this lens is possible not only for rays, but also for waves. Conversely, if at least one of the ratios $a/b, b/c, a/c$ is irrational, rays will not form closed curves, and a wave released from any point from within the lens will never reform its original shape.

5. Conclusion

In conclusion, we have presented a class of absolute optical instruments where light rays trace out Lissajous figures and imaging is stigmatic everywhere within the lenses. Unlike in the previously known absolute instruments, the source, its image and the center of the lens do not have to lie on a straight line. Whether other lenses exist with this property or whether this lens is unique remains an open question.

Acknowledgements

A. Danner acknowledges the Tier I AcRF Award R263000690112 from Ministry of Education, Singapore; H. L. Dao acknowledges the grant NRF-CRP 4-2008-06 from National Research Foundation - Prime Minister's office, Singapore; T. Tyc acknowledges support of the grant P201/12/G028 of the Czech Science Foundation, and of the QUEST program grant of the Engineering and Physical Sciences Research Council.